

Lithium-salt-based deep eutectic solvents: Importance of glass formation and rotation-translation coupling for the ionic charge transport

A. Schulz, P. Lunkenheimer^{a)}, and A. Loidl

AFFILIATIONS

Experimental Physics V, Center for Electronic Correlations and Magnetism, University of Augsburg, 86135 Augsburg, Germany

^{a)}Author to whom correspondence should be addressed: peter.lunkenheimer@physik.uni-augsburg.de

ABSTRACT

Lithium-salt-based deep eutectic solvents, where the only cation is Li^+ , are promising candidates as electrolytes in electrochemical energy-storage devices like batteries. We have performed broadband dielectric spectroscopy on three such systems, covering a broad temperature and dynamic range that extends from the low-viscosity liquid around room temperature down to the glassy state approaching the glass-transition temperature. We detect a relaxational process that can be ascribed to dipolar reorientational dynamics and exhibits the clear signatures of glassy freezing. We find that the temperature dependence of the ionic dc conductivity and its room-temperature value also are governed by the glassy dynamics of these systems, depending, e.g., on the glass-transition temperature and fragility. Compared to the previously investigated corresponding systems, containing choline chloride instead of a lithium salt, both the reorientational and ionic dynamics are significantly reduced due to variations of the glass-transition temperature and the higher ionic potential of the lithium ions. These lithium-based deep eutectic solvents partly exhibit significant decoupling of the dipolar reorientational and the ionic translational dynamics and approximately follow a fractional Debye-Stokes-Einstein relation, leading to an enhancement of the dc conductivity, especially at low temperatures. The presented results clearly reveal the importance of decoupling effects and of the typical glass-forming properties of these systems for the technically relevant room-temperature conductivity.

I. INTRODUCTION

Deep eutectic solvents (DES) have come into the focus of recent research as their properties make them promising candidates for numerous applications, e.g., in material synthesis or electrochemical devices.^{1,2,3,4,5,6,7,8,9,10,11} Most DESs are easy to produce, sustainable, and biocompatible, partly being even composed of constituents found in nature. Thus, they turn out to be "greener" alternatives to ionic liquids, considered for similar applications.

As in all eutectics, in DESs a melting-point reduction arises due to the mixing of two or more components, making them liquid at room temperature. In the most common class of DESs, these components are molecular hydrogen-bond donors (HBD) like glycerol or urea, mixed with a salt acting as hydrogen-bond acceptor. The latter commonly is a quaternary ammonium salt, like in the often-investigated DESs glyceline, ethaline, and reline, which are mixtures of choline chloride with glycerol, ethylene glycol, or urea, respectively, all with 1:2 molar ratio. Their large salt fraction leads to considerable ionic conductivity, a prerequisite for electrochemical applications. However, for these applications, the most prominent one being electrolytes in batteries, usually the presence of ions like Li^+ or Na^+ is required. In DESs as those discussed above, this can be achieved by admixing salts like

lithium bis(trifluoromethane)sulfonimide (LiTFSI) or LiPF_6 .⁹ An alternative approach is the investigation of DESs where the only cation is Li^+ or Na^+ . This avoids the possible accumulation of the large cations (e.g., choline⁺) at the electrode, blocking it for the Li^+ ions.¹² For example, in a molecular-dynamics study, urea mixed with LiTFSI was proposed to be a promising DES for electrochemical applications.¹³ Indeed, in an earlier work,¹⁴ relatively high dc conductivities were detected in this system. The existence of Li-salt-based DESs was also reported for the common HBDs glycerol and ethylene glycol, e.g., in Refs. 15 and 16.

The application of DESs as electrolytes in electrochemical devices requires a high ionic dc conductivity, σ_{dc} , beyond about $10^{-4} \Omega^{-1}\text{cm}^{-1}$ at room temperature. To optimize the conductivity and to understand the considerable variation of σ_{dc} of different DESs,^{5,9,12,15,23} a better knowledge of the ionic and molecular motions within these materials is desirable. For this purpose, dielectric spectroscopy is a well-suited experimental method as it can simultaneously provide information on the translational ionic and the reorientational molecular motions.^{17,18} In DESs, the latter arise because the HBDs usually are asymmetric molecules with rotational degrees of freedom and in many cases, this is also the case for at least one of the added ion species. Several previous works have revealed that the reorientational molecular motions,

present in certain ionic conductors, including ionic liquids and superionic and plastic crystals, seem to be highly relevant for ionic mobility.^{19,20,21,22} Interestingly, consistent with this notion, for the DESs glyceline and ethaline, we recently found a close correlation of their ionic dc conductivity with the reorientational dynamics as detected by dielectric spectroscopy.²³ However, for reline some minor but significant deviations showed up.

Moreover, dielectric spectroscopy is also able to obtain valuable information on the glass transition, often occurring for eutectic mixtures at low temperatures. Indeed, many DESs seem to be glass-forming liquids^{4,24} but, overall, this phenomenon is only rarely investigated in this material class. In a previous work,²³ we found that the temperature dependence of both the rotational and ionic dynamics of glyceline, ethaline, and reline indeed reveal the characteristics of glassy freezing. This also affects their room-temperature properties, e.g., the dc conductivity strongly depends on the glass-transition temperature.

In the present work, we report the results of broadband dielectric spectroscopy on three Li-salt-based DESs, with the same HBDs as the previously investigated^{23,25} glyceline, ethaline, and reline. We especially treat the question of the possible coupling of the translational and reorientational dynamics in these systems and their glassy freezing. It should be noted that so far there are only few earlier dielectric investigations of DESs^{16,23,24,26,27,28,29,30} often not addressing the reorientational dynamics, and, to our knowledge, none of them has tackled the technically relevant, purely Li-salt-based DESs.

II. Experimental Details

The two salts LiTFSI and lithium triflate (LiOTf), as well as glycerol, were purchased from Sigma Aldrich, while urea and ethylene glycol are obtained from Alfa Aesar. The first DES, denoted LiTFSI/urea (LiTFSI + urea, 1:3.1 molar ratio), was prepared along the lines of Ref. 14 by blending appropriate amounts of the components inside a glass vessel and vacuum drying the mixture for 6.5 hours at 375 K. This way, any significant water entrapments were removed, while the source materials were thoroughly mixed. Similarly, LiOTf/Gly (LiOTf + glycerol, 1:3 molar ratio) and LiOTf/EG (LiOTf + ethylene glycol, 1:4 molar ratio) were produced, as described in Ref. 15, by heating the mixtures of the starting materials at 355 K for around 20 hours. All three DESs appeared as colorless, translucent, and homogeneous liquids with LiOTf/EG exhibiting a noticeably lower viscosity, compared to the other two solvents. The water content of all samples was tested by coulometric Karl-Fischer-Titration and determined to be 0.52, 0.01, and 0.21 wt% for LiOTf/Gly, LiOTf/EG, and LiTFSI/urea, respectively. To prevent water uptake, during the measurements the samples were kept in a dry nitrogen atmosphere. To cover a broad frequency range from about 1 Hz to 1 GHz, the dielectric measurements were performed with two different techniques, frequency-response analysis ($\nu < 3$ MHz) and coaxial reflectometry³¹ ($\nu > 1$ MHz). For more information, the reader is referred to Ref. 23. Furthermore, differential scanning calorimetry (DSC) measurements were conducted using a DSC 8500 from

PerkinElmer at a scanning rate of 10 K/min during heating and cooling. The onset of the step-like increase of the heating data revealed the glass-transition temperatures of the three eutectic mixtures.

III. RESULTS AND DISCUSSION

A. Dielectric spectra

There are various ways to represent and evaluate the results of dielectric measurements of ionically conducting systems. Often such data are analyzed in terms of the dielectric modulus. However, as discussed, e.g., in Ref. 32, for systems with simultaneous reorientational and translational motions some problems may occur for this representation. Indeed, the original modulus formalism is intended for "ionic conductors which contain no permanent molecular dipoles".³³ Thus, here we follow the approach in our earlier works on DESs^{23,25,32} and ionic liquids,²² analyzing the complex dielectric permittivity, $\epsilon^* = \epsilon' - i\epsilon''$, which is the natural representation for materials with reorientational degrees of freedom and also allows for a direct comparison with our previous results on glyceline, ethaline, and reline.^{23,32} In addition, we provide the real part of the conductivity σ' , which is proportional to $\epsilon''\nu$ and enables the direct identification of the dc conductivity.

Figure 1 shows spectra of the dielectric constant (ϵ'), loss (ϵ'') and conductivity (σ') as obtained for LiOTf/Gly at various temperatures. Overall, these spectra are qualitatively similar to those reported for the corresponding choline-chloride-based DESs with the same HBDs.^{23,32} The increase of $\epsilon'(\nu)$ [Fig. 1(a)] to unreasonably high values, exceeding 10^6 , observed at low frequencies and high temperatures, is due to electrode polarization.³⁴ This non-intrinsic phenomenon is a common finding for ionic conductors. It also explains the low-frequency decrease of $\sigma'(\nu)$ detected at the highest temperatures [Fig. 1(c)],³⁵ and (due to the relation $\epsilon'' \propto \sigma'/\nu$) the corresponding more shallow $\epsilon''(\nu)$ trace, e.g., observed below about 100 Hz for the 286 K curve [Fig. 1(b)]. At frequencies beyond the electrode-dominated regime, the ϵ' spectra reveal the typical indications of a dipolar relaxation process, signified by a step-like decrease with increasing frequency (see inset of Fig. 1 for a zoomed view). The points of inflection of these steps strongly shift to lower frequencies upon cooling, typical for the slowing down of the dynamics found in glass-forming materials.^{18,36} At room temperature, the relaxation step in $\epsilon'(\nu)$ is located at roughly 100 MHz. This is of similar order as reported for pure glycerol,³⁶ in agreement with the findings for glyceline.^{23,37} Thus, reorientations of the glycerol molecules, representing 75% of the sample constituents, can be assumed to play a major role in the generation of the relaxation process observed in this DES. The second dipolar entity in this DES, LiOTf, does not lead to a separate relaxation process in the spectra and probably its rotations are closely coupled to those of glycerol. The detection of only a single relaxation process for mixtures of two types of dipoles is an often-found phenomenon.^{38,39}

In general, relaxation steps in $\epsilon'(\nu)$ should be accompanied by relaxation peaks in $\epsilon''(\nu)$. However, as often found for systems with relatively high conductivity, in the present case these peaks are partly superimposed by the strong dc-

conductivity contribution in the loss spectra, $\varepsilon''_{dc} \propto \sigma_{dc}/\nu$, which leads to a $1/\nu$ increase towards lower frequencies. Therefore, only the right flanks of the expected peaks show up, which, at high frequencies, give rise to a shallower decrease of $\varepsilon''(\nu)$, compared to the dc contribution [cf. the dashed line in Fig. 1(b) indicating the unobscured relaxation peak as obtained from the fits described below]. A derivative analysis of $\varepsilon'(\nu)$ as proposed in Ref. 40 and previously performed for glycine³² supports this notion.

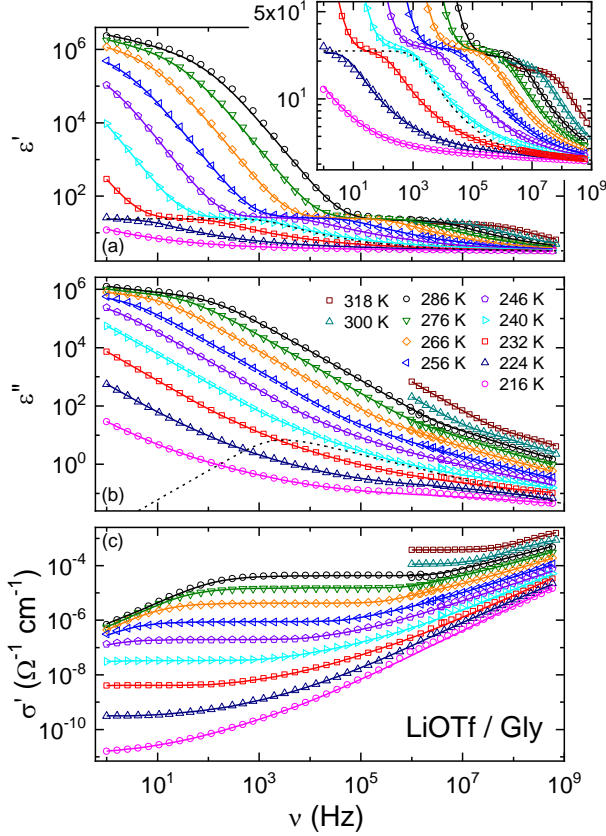


FIG. 1. Frequency dependence of the dielectric constant ε' (a), the dielectric loss ε'' (b), and the real part of the conductivity σ' (c), measured at various temperatures for LiOTf/Gly. For the two highest temperatures, only measurements with the high-frequency device are provided ($\nu \geq 1$ MHz), which is sufficient to reveal the dc conductivity and dipolar relaxation. The inset shows a zoomed view of the intrinsic relaxation steps in $\varepsilon'(\nu)$. The solid lines in (a) and (b) are fits with an equivalent circuit, assuming a distributed RC circuit to describe the blocking electrodes,³⁴ intrinsic relaxation processes (α and secondary), and a contribution from dc-conductivity as described in the text. The real and imaginary parts of the permittivity were fitted simultaneously and the fits of the conductivity were calculated using $\sigma' = \varepsilon'' \varepsilon_0 \omega$. As an example, the dashed lines in (a), (b), and in the inset show the contribution of the α relaxation for 240 K.

At the lowest temperature in Fig. 1, where the relaxation step in $\varepsilon'(\nu)$ has essentially shifted out of the frequency window, the loss spectrum in Fig. 1(b) reveals a region with weak frequency dependence at high frequencies (e.g., at $\nu > 10^5$ Hz for 216 K). This points to further minor contributions in this region, e.g., due to secondary processes, usually termed β relaxations, which are common phenomena of dipolar glass-forming liquids,^{41,42,43} including ionically

conducting systems.^{22,23,44} The discussion of these effects is out of the scope of the present work and these low-temperature spectra provide neither any information on the main reorientational process (termed α relaxation) nor on the dc conductivity.

The ionic dc conductivity of LiOTf/Gly is signified by the frequency-independent plateaus in $\sigma'(\nu)$ at frequencies beyond the mentioned electrode-dominated regime [Fig. 1(c)]. Its absolute value strongly decreases with decreasing temperature, mirroring the essentially thermally-activated nature of the ionic charge transport. At higher frequencies, the dc plateau crosses over into a region with increasing $\sigma'(\nu)$. This mirrors the mentioned relaxational response (the right flanks of the α -relaxation peaks) as detected in $\varepsilon''(\nu)$, contributing to the conductivity spectra due to the close relation of both quantities ($\sigma \propto \varepsilon''\nu$).

Here it seems worth mentioning that this reasoning departs from the canonical interpretation given in the majority of literature on the frequency-dependent conductivity in ionic conductors, where the mentioned crossover mirrors the transition from the dc to ac conductivity. According to this interpretation, the data as shown in Fig. 1 are analyzed in terms of purely translational charge transport via ion hopping, without assuming any contributions from dipolar reorientation dynamics. A prominent example is the random free-energy barrier hopping model (RBM),^{45,46} which predicts a relaxation step in $\varepsilon'(\nu)$ that arises from local ion motions. It was previously applied, e.g., to two DES systems²⁴ and several ionic liquids.^{47,48,49} Within this framework, the mentioned increase of $\sigma'(\nu)$ at high frequencies is due to ac conductivity arising from hopping charge transport. On the other hand, as argued in Refs. 23 and 32 and discussed above, it is clear that the well-known reorientational motions of the HBDs, making up 75 - 80 mol% of the investigated DESs, should lead to significant relaxational signatures in the spectra. Of course, it cannot be excluded that contributions from ion hopping and dipolar reorientations superimpose in the measured data. However, as we will see below and as also found in our previous works,^{23,32} the DES spectra can be explained without invoking any additional ac-conductivity contributions or relaxational response arising from ionic charge transport, whose only contribution to the spectra seems to be the dc conductivity. Therefore, in light of Occam's razor, here we describe our data exclusively by reorientational dynamics (which inevitably has to exist in these materials) and dc charge transport. In Ref. 32, the feasibility of an approach combining the RBM prediction and dipolar reorientation dynamics was demonstrated, but the increased number of parameters and problematic deconvolution of the different spectral contributions makes it difficult to arrive at definite conclusions in this way for the present samples.

Figures 2 and 3 show the dielectric spectra of LiOTf/EG and LiTFSI/urea.⁵⁰ The upper frames provide a zoomed view of the intrinsic relaxation steps in $\varepsilon'(\nu)$. With the typical signatures of electrode polarization, an intrinsic relaxation process in $\varepsilon'(\nu)$ and the dc plateau in $\sigma'(\nu)$, they qualitatively resemble those of LiOTf/Gly in Fig. 1. Especially for LiOTf/EG, at the lowest temperatures a weak broad loss peak or shoulder [e.g., around 10^4 Hz in the 171 K curve in Fig. 2(b)] is unequivocally detected. This confirms the β -relaxation

scenario discussed above to explain the nearly frequency-independent loss observed at low temperatures.

To fit the data of Figs. 1-3, we formally describe the electrode polarization effects by a distributed RC circuit connected in series to the bulk sample,³⁴ as previously employed for DESs and other ionic conductors.^{21,22,23,32} For the α relaxation, we use the Cole-Davidson (CD) formula⁵¹ and the secondary relaxation is fitted by the Cole-Cole (CC) function,⁵² both commonly-used empirical fit functions of α and secondary processes, respectively.^{17,18,43} Finally, the dc-conductivity contribution to the loss is accounted for by $\varepsilon''_{dc} = \sigma_{dc}/(\varepsilon_0 \omega)$ (with ε_0 the permittivity of free space and $\omega = 2\pi\nu$). The solid lines in Figs. 1-3 show fits with this approach, simultaneously performed for $\varepsilon'(\nu)$ and $\varepsilon''(\nu)$. Just as for the choline-chloride-based DESs,^{23,32} the experimental spectra can be well fitted in this way. Only for LiTFSI/urea, we found that two CC functions had to be employed to properly fit the high-frequency part of the low-temperature curves at $T \leq 244$ K. We want to point out that, depending on temperature, only part of the different contributions had to be employed for the fits, thus avoiding an excessive number of fit parameters. For example, at low temperatures, the electrode effects can be neglected and at high temperatures, the secondary relaxations play no role.

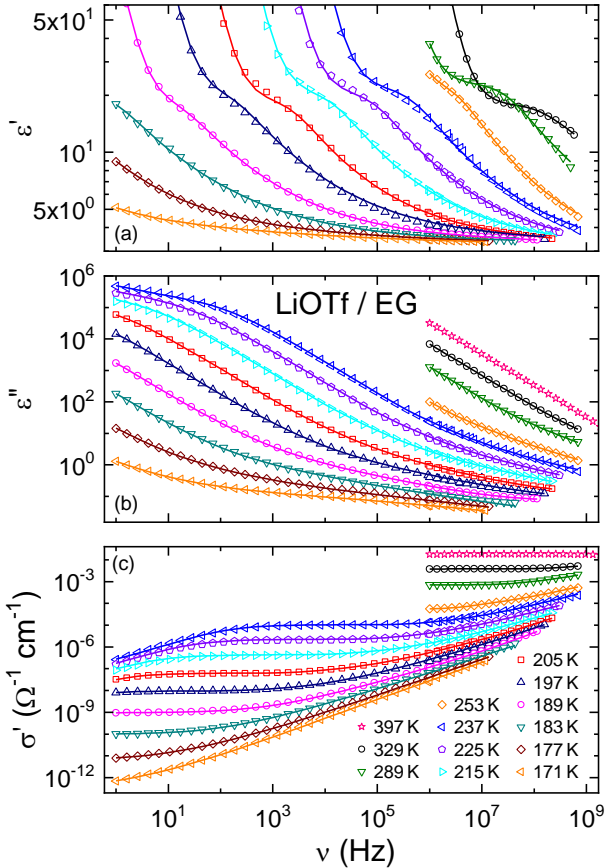


FIG. 2. Dielectric response of LiOTf/EG [corresponding plot as in Fig. 1 but with frame (a) providing a zoomed view of the intrinsic α relaxation]. The solid lines have the same meaning as in Fig. 1. For 397 K, no meaningful results could be obtained for ε' , due to the high conductivity at this temperature.

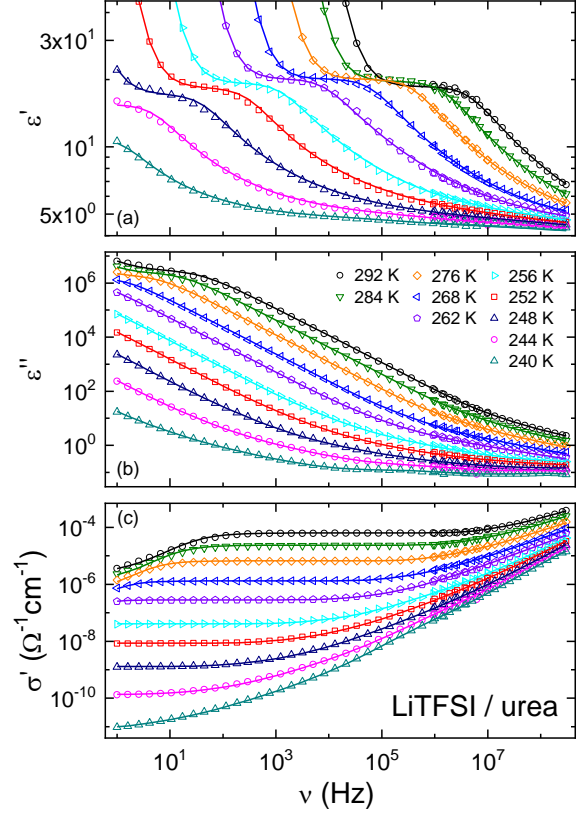


FIG. 3. Dielectric response of LiTFSI/urea (corresponding plot as in Fig. 2). The solid lines have the same meaning as in Figs. 1 and 2.

B. Dc conductivity and α -relaxation time

From an application point of view, the dc conductivity of these systems, reaching technically relevant values of $> 10^{-4} \Omega^{-1}\text{cm}^{-1}$ at room temperature,^{14,15,16} is the most interesting quantity. The temperature-dependent dc conductivities of the investigated DESs as resulting from the fits in Figs. 1-3 are shown in Fig. 4(a) using an Arrhenius representation (closed symbols). In all samples, we find clear deviations from a simple thermally-activated temperature dependence. This is typical for glass-forming ionic conductors^{21,22,53} and mirrors the general non-Arrhenius behavior, characteristic of the structural dynamics of glass-forming liquids. While the $\sigma_{dc}(T)$ traces of the three investigated DESs approach each other at high temperatures, at low temperatures their dc-conductivity values deviate by many decades. As previously reported for ethaline, glyceline, and reline [open symbols shown for comparison in Fig. 4(a)²³], for the HBD ethylene glycol the highest and for the HBD urea the lowest conductivity is detected. These low-temperature deviations seem to be directly related to the different glass-transition temperatures T_g of these systems determined by DSC, which are 175, 208, and 239 K for LiOTf/EG, LiOTf/Gly, and LiTFSI/urea, and 155, 175, and 205 K for ethaline, glyceline, and reline,²³ respectively. Having in mind the simple picture of particles diffusing through a viscous medium, it is reasonable that the strongly increasing viscosity $\eta(T)$ when approaching T_g ,⁵⁴

accompanied by a slowing down of molecular dynamics, causes a reduction of the ionic mobility.

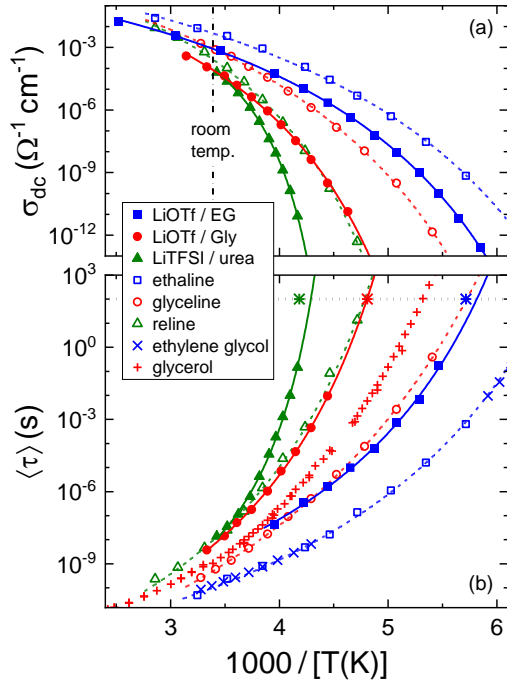


FIG. 4. Arrhenius plot of the dc conductivity (a) and mean α -relaxation time (b) for the DESs investigated in the present work and in Ref. 23. In addition, in (b) also $\tau(T)$ data for the pure HBDs glycerol⁶⁹ (plusses) and ethylene glycol²³ (crosses) are included, as well as glass-transition temperatures for the lithium-salt-based DESs (stars) obtained via DSC measurements. The solid and dashed lines in (a) and (b) are fits with the VFT law, Eqs. (1) or (2), respectively. The vertical dash-dotted line in (a) indicates room temperature (295 K). The horizontal dotted line in (b) denotes $\tau(T_g) = 100$ s, which enables a rough estimate of the glass-transition temperature.

Another notable effect revealed by Fig. 4(a) are the systematic differences between the DESs containing lithium salts and those with the same HBDs but containing the choline-chloride salt instead (cf. closed and open symbols with the same color). In all three cases, the lithium systems exhibit significantly lower conductivities. These differences are most pronounced at low temperatures but, at least for LiOTf/EG and LiOTf/Gly, persist up to the highest investigated temperatures. As the Li^+ ions are by far smaller than the choline and chlorine ions, naively a higher mobility and, thus, higher conductivity could be expected for these ions. However, again different glass temperatures for the choline-chloride and Li-salt-based systems seem to at least partly explain the much lower σ_{dc} of the latter, especially at low temperatures. The small size of the lithium ion causes a higher ionic potential (ratio of charge to ion radius) than for both the cation and anion in choline-chloride. This should give rise to stronger inter-ionic interactions and also enhance the interactions between the Li^+ ions and the HBD molecules. It seems that this causes a strengthening of the local, transient structural network within the liquid, which leads to higher viscosity at a given temperature and, thus, to an increased glass-transition temperature. Of course, the stronger interactions of the lithium ions amongst each other and with the other constituents also should directly reduce their

mobility, without invoking a viscosity variation, which may explain the observed persistence of the conductivity differences up to high temperatures, far above T_g . A reduction of ionic conductivity due to the replacement of larger by smaller ions is a well-known phenomenon and was, e.g., reported for ionic liquids in Refs. 47 and 55.

TABLE I. Glass-transition temperatures as determined from DSC measurements and parameters obtained from the VFT fits of $\sigma_{dc}(T)$ and $\langle\tau\rangle(T)$ shown in Fig. 4 and the fragility parameter calculated from D_τ .

	T_g (K)	$T_{VF\sigma}$ (K)	D_σ	σ_0 ($\Omega^{-1}\text{cm}^{-1}$)	$T_{VF\tau}$ (K)	D_τ	τ_0 (s)	m
LiOTf/EG	175	122	12.4	5.3	128	11.4	4.8×10^{-13}	68
LiOTf/Gly	208	154	11.5	22	157	12.3	5.2×10^{-15}	64
LiTFSI/urea	239	208	4.1	1.4	203	5.2	7.9×10^{-14}	129

Just as previously found for ethaline, glyceline, and reline,²³ $\sigma_{dc}(T)$ of the present lithium-salt DESs can be reasonably well fitted by a modification of the empirical Vogel-Fulcher-Tammann (VFT) law^{56,57,58} [lines in Fig. 4(a)]:

$$\sigma_{dc} = \sigma_0 \exp \left[\frac{-D_\sigma T_{VF\sigma}}{T - T_{VF\sigma}} \right] \quad (1)$$

Here σ_0 is a prefactor, D_σ is the so-called strength parameter, which quantifies the deviations from Arrhenius behavior,⁵⁹ and $T_{VF\sigma}$ is the Vogel-Fulcher temperature where σ_{dc} approaches zero. The resulting fit parameters are listed in Table I.

Figure 4(b) shows an Arrhenius plot of the average reorientational α -relaxation times $\langle\tau\rangle(T)$ (closed symbols), calculated from the parameters of the CD function⁶⁰ which was used for describing the α relaxation in the fits of the dielectric spectra. The open symbols again denote the results for the corresponding choline-chloride-based DESs.^{23,25} Just as for $\sigma_{dc}(T)$, quantifying the translational ionic dynamics [Fig. 4(a)], the temperature dependence of $\langle\tau\rangle$, related to the dipolar reorientational dynamics, exhibits marked deviations from Arrhenius behavior, typical for glass-forming liquids.^{17,18,36,61,62} The relaxation-time curves of Fig. 4(b) roughly appear like mirror images of the $\sigma_{dc}(T)$ curves in Fig. 4(a) and show corresponding variations, with LiTFSI/urea having the highest and LiOTf/EG the lowest $\langle\tau\rangle$ values among the lithium systems at a given temperature. The Li-salt systems exhibit systematically longer relaxation times than the choline-chloride ones with the same HBDs [cf. closed and open symbols in Fig. 4(b)]. Again, all these variations may partly be ascribed to the different glass temperatures of these systems, having in mind the simple picture of asymmetric particles rotating within a viscous medium. In general, a comparison of Figs. 4(a) and (b) reveals that both the ionic translational and the dipolar reorientational dynamics are at least roughly coupled. Similar coupling was previously stated for glyceline, ethaline, and reline²³ and very recently demonstrated to be mainly mediated by the viscosity with certain deviations for reline.³² It will be treated in more detail below.

As shown by the solid lines in Fig. 4(b), $\langle\tau\rangle(T)$ of the three investigated DESs can be well fitted by the VFT law, Eq. (2),^{56,57,58,59} again typical for supercooled liquids.

$$\langle\tau\rangle = \tau_0 \exp \left[\frac{D_\tau T_{VFT}}{T - T_{VFT}} \right] \quad (2)$$

The resulting parameters are listed in Table I. The strength parameters and Vogel-Fulcher temperatures from the fits of $\sigma_{dc}(T)$ and $\langle\tau\rangle(T)$ are of comparable order (Table I), again pointing to a certain coupling of the ionic and reorientational dynamics. From D_τ the fragility parameter m can be calculated (Table I), which is an often-used measure of the deviations of $\langle\tau\rangle(T)$ from Arrhenius behavior.⁶³ We obtain values of 68, 64, and 129 for LiOTf/EG, LiOTf/Gly, and LiTFSI/urea, respectively. Within the strong-fragile classification of glass-forming liquids,⁵⁹ this characterizes the present DESs as intermediate to fragile. In general, the fragility of a glass-forming ionic conductor has an influence on its room-temperature conductivity as demonstrated for ionic liquids in Ref. 64. In the present case, e.g., the significantly lower D_σ of the urea system corresponds to a more pronounced bending in its $\sigma_{dc}(T)$ curve in Fig. 4(a). This leads to an enhancement of its conductivity at room temperature, which becomes comparable to that of LiOTf/Gly despite the higher glass temperature of LiTFSI/urea. The reason for the higher fragility of the urea systems is unclear. One may speculate that rather complex ion-HBD aggregations as found for reline⁶⁵ could also exist in LiTFSI/urea, leading to a more complex energy landscape and, thus, higher fragility.^{66,67}

To estimate the glass-transition temperature, often the criterion $\langle\tau\rangle(T_g) \approx 100$ s is used. Extrapolating the fit curves in Fig. 4(b), we arrive at 172, 208, and 233 K for LiOTf/EG, LiOTf/Gly, and LiTFSI/urea, respectively. As mentioned above, from DSC experiments we have obtained 175, 208,⁶⁸ and 239 K, respectively (Table I). For the ethylene-glycole and glycerol systems, the agreement is reasonable. The 6 K lower T_g from the $\langle\tau\rangle(T)$ data, found for LiTFSI/urea, could indicate slightly decoupled, enhanced reorientational dynamics at low temperatures. Further investigations are necessary to clarify this issue.

For the HBD glycerol, relaxation-time data are available in a broad temperature range as shown by the plusses in Fig. 4(b).⁶⁹ Remarkably, while the admixture of choline chloride to glycerol leads to an acceleration of reorientational motions especially at low temperatures, signified by a reduction of the relaxation times (open circles),²³ for LiOTf we find a slowing down (closed circles). The latter was also reported for the admixture of LiCl to glycerol.⁷⁰ In general, it is plausible that the addition of ions partially breaks up the intermolecular hydrogen-bond network of pure glycerol. Our results suggest that, for the relatively large ions in glyceline, this weakens the structural network, which leads to faster molecular dynamics, including the reorientational motions characterized by $\langle\tau\rangle$. In contrast, the much smaller radius of the lithium ions, causing a high ionic potential, seems to give rise to stronger interactions and a slowing down of the dynamics, roughly speaking by partly replacing the hydrogen bonds with stronger ionic bonds. While these simple considerations seem plausible, one should be aware that complex aggregations between the ions and HBD molecules as reported for the

choline-chloride-based DESs^{65,71,72,73} are likely to also exist in the Li-salt systems. This should affect both, the dipolar reorientational and the ionic translational [Fig. 4(a)] dynamics. Further work, e.g., using nuclear magnetic resonance measurements, are necessary to clarify the role of such aggregates for the molecular and ionic dynamics in this class of DESs.

For the HBD ethylene glycol, temperature-dependent relaxation-time data are available, too.^{23,74,75} Those from Ref. 23 are shown by the crosses (×) in Fig. 4(b). Just as for glycerol, the addition of a lithium salt leads to considerable slowing down of the reorientational motions [cf. crosses and closed squares in Fig. 4(b)]. However, as already noted in Ref. 23, in this case, the admixing of choline chloride to ethylene glycol does not significantly alter the relaxation time (cf. crosses and open squares), in marked contrast to glycerol. In light of the discussion in the previous paragraph, this would imply that the bonding within the structural network of the HBD molecules has similar strength both in pure ethylene glycol and ethaline. Notably, the ethylene glycol molecule only comprises two OH groups instead of three in glycerol. In the pure HBD, this should lead to a qualitatively different network that is less three-dimensionally interconnected than for glycerol. This weaker network seems to be less affected by the addition of large ions. Finally, for pure urea, only a single relaxation time in the melt at 406 K was reported in literature²⁹ precluding any statements about the influence of ion admixture.

C. Coupling of reorientational and translational dynamics

In Ref. 23, for ethaline and glyceline nearly perfect coupling of the dipolar reorientational dynamics and the translational ion dynamics was evidenced by the identical temperature dependences of $\langle\tau\rangle$ and $\rho_{dc} = 1/\sigma_{dc}$, implying $\langle\tau\rangle \propto \rho_{dc}$.⁷⁶ In contrast, in reline weak but significant decoupling showed up. For the present Li-salt-based DESs, this coupling is examined in Fig. 5, where, for each material, the logarithms of both quantities are shown within the same frame, thereby ensuring the same number of decades on the two ordinates. Then, by properly choosing the starting values of the y-axes, a perfect match of the two curves would indicate direct proportionality of both quantities. Figure 5 reveals that $\langle\tau\rangle$ and ρ_{dc} of the present DESs in general exhibit similar temperature dependence as already suggested by a comparison of Figs. 4(a) and (b). However, in contrast to ethaline and glyceline,^{23,32} especially for LiOTf/Gly and LiOTf/EG small but significant decoupling effects show up while for the urea-based sample a better match of both quantities can be achieved in this way. In Fig. 5, we adjusted the y-axes to reach an agreement at the highest covered temperature, because at high temperatures decoupling effects usually are least pronounced. $\langle\tau\rangle(T)$ and $\rho_{dc}(T)$ in LiOTf/Gly and LiOTf/EG show growing differences with decreasing temperature, finally reaching about one decade. In this respect, these materials resemble the behavior previously found for reline.²³ Interestingly, for the latter very recent viscosity measurements in a broad temperature range revealed that the reorientational motions are well coupled to the viscosity while the ionic motions are

decoupled from both dynamics.³² Corresponding viscosity measurements are necessary to clarify whether a similar scenario applies for the present Li-salt DESs and to help clarifying the better coupling found for LiTFSI/urea.

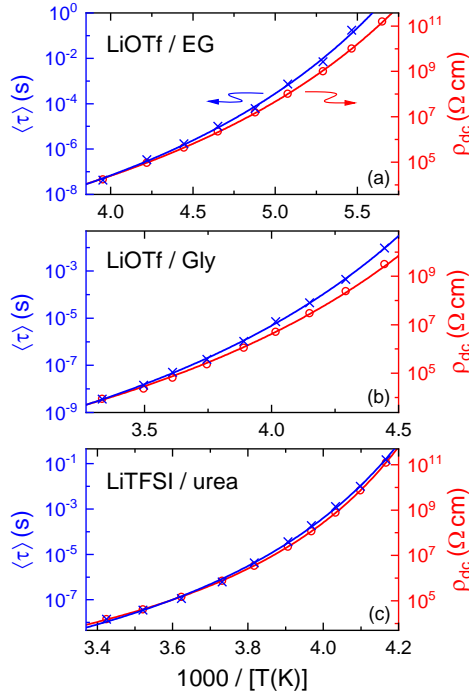


FIG. 5. Arrhenius plots of the average α -relaxation times (crosses, left ordinates) and the dc resistivities (circles, right ordinates) of the investigated DESs. For each frame, the number of decades covered by the left and right ordinates is identical. Their starting values were adjusted to achieve a match of the two quantities at the highest investigated temperature. The lines are fits with the VFT law [same as in Fig. 4(a)], taking into account $\rho_{dc} = 1/\sigma_{dc}$.

In Ref. 32, for glyceline, ethaline, and reline nearly perfect reorientation-viscosity coupling was found. If it also applies to the present systems, the crosses in Fig. 5 characterizing the reorientational dynamics also provide an estimate of the temperature dependence of the viscosity. Then the results of Fig. 5 imply that at low temperatures the ionic mobility of LiOTf/EG and LiOTf/Gly is enhanced compared to the naive picture of a sphere that translationally moves within a viscous medium. In any case, the decoupling effects observed in Figs. 5(a) and (b) demonstrate that a revolving-door-like scenario,^{20,21,77} where the rotation of the dipoles opens up paths for the translational motions of the ions, is not the dominant charge-transport process in these two materials. This mechanism should lead to good coupling of reorientational and ionic translational motions (i.e., $\langle \tau \rangle \propto \rho_{dc}$) as found for plastic crystals,^{20,21} various ionic liquids,²² and also for glyceline and ethaline^{23,32} but which is not fulfilled for two of the present DESs (Fig. 5). It should be noted that for many plastic crystals the applicability of the revolving-door mechanism is quite evident,^{20,21,77} and for ionic liquids it also seems likely.²² However, for the DESs glyceline and ethaline the results can also be explained by rotation-translation coupling via the viscosity.³² In general, deviations from $\langle \tau \rangle \propto \rho_{dc}$ exclude dominant revolving-door charge transport

but the validity of this proportionality in a material may also be explained without invoking this mechanism.

As mentioned above, for the choline-chloride-based DESs, good coupling of ionic and rotational motions was found for the HBDs ethylene glycol and glycerol, but some decoupling showed up for urea.²³ It is puzzling that in the present Li-salt-based DESs the situation is just the other way round, i.e., rather good coupling arises for the urea system and worse coupling for EG and glycerol (Fig. 5). The urea molecule differs by having hydrogen-bonding NH_2 and carbonyl groups instead of the hydroxyl groups of the alcohol HBDs, but it is unclear how this affects the coupling.

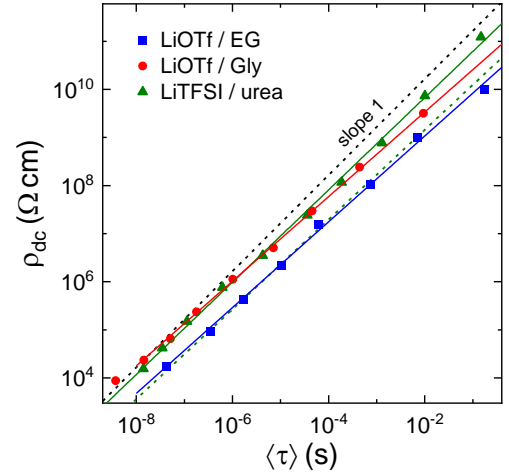


FIG. 6. Variation of the dc resistivities of the three investigated DESs with their reorientational relaxation times shown in a double-logarithmic plot. The upper dashed line with slope one indicates linear behavior, $\rho_{dc} \propto \langle \tau \rangle$, and represents the previously used fit curve describing the glyceline and ethaline data.²³ The solid lines are fractional power laws $\rho_{dc} \propto \langle \tau \rangle^\xi$, approximating the present systems. The lower dashed line shows the power law employed for fits of the reline data in Ref. 23.

Finally, Fig. 6 shows the variation of the dc resistivity with the α -relaxation time (obtained at different temperatures) for the investigated DESs. As noted in Ref. 23, for glyceline and ethaline $\rho_{dc} \propto \langle \tau \rangle$ is valid (upper dashed line with slope 1 in Fig. 6), in accord with the so-called Debye-Stokes-Einstein (DSE) relation.^{78,79,80,81} In contrast, for reline a fractional power law was found, $\rho_{dc} \propto \langle \tau \rangle^\xi$ with $\xi = 0.93$ (lower dashed line). It reminds of the fractional DSE behavior reported for various glass-forming systems.^{78,79} As already suggested by Fig. 5, the Li-salt-based DESs investigated in the present work also significantly deviate from the DSE relation. Indeed, like reline they follow fractional power laws with $\xi = 0.89, 0.88$, and 0.96 for LiOTf/EG, LiOTf/Gly, and LiTFSI/urea, respectively (solid lines in Fig. 6). Once again, the urea-based DES displays a different behavior, compared to the other two systems. In agreement with the rather good match of the two curves in Fig. 5(c), the exponent ξ is close to one for this DES. Figure 6 reveals that, especially at low temperatures, LiOTf/Gly and LiTFSI/urea have clearly enhanced dc conductivity (reduced dc resistivity) for a given relaxation time and probably also for a given viscosity when assuming the mentioned reorientation-viscosity coupling.³² However,

one should be aware that their conductivities for a given *temperature* are lower than for the choline-chloride DESs. Notably, without the decoupling evidenced by the fractional DSE relation, σ_{dc} of these systems would be even lower.

IV. SUMMARY AND CONCLUSIONS

In summary, we have performed broadband dielectric spectroscopy measurements on three DESs where the hydrogen-bond acceptor is a lithium salt. These measurements cover a broad dynamic range extending from the low-viscosity liquid around room temperature well into the supercooled-liquid state and finally approaching the glass state close to T_g . Just as for the previously investigated systems, composed of the same HBDs but containing choline chloride instead of a lithium salt, we find the signatures of a dipolar relaxation process revealing the characteristics of glassy freezing, in particular pronounced non-Arrhenius behavior. The HBDs represent the by far largest fraction of these DESs and the pure HBDs all have well-pronounced relaxation processes due to dipolar reorientations, whose relaxation times at high temperatures are of similar order as the present ones.^{23,26,36,69,74,75} Therefore it is reasonable to assume that the detected relaxation process is predominantly due to reorientational motions of the HBD molecules. We find that, in general, for the investigated Li-salt-based DESs this dynamics is slower than for the corresponding choline-chloride systems and also slower than for the pure HBDs, especially at low temperatures. These findings and the detected strong relaxation-time differences between the three DESs can be rationalized by variations in the glass-transition temperature and/or the high ionic potential of the added lithium ions.

The temperature dependence of the technically relevant dc conductivities of these lithium DESs also reveals clear non-Arrhenius behavior, indicating that the translational ionic dynamics in principle is governed by the same glassy freezing as evidenced by the reorientational relaxation times. Analogous to the observed slowing down of the reorientational dynamics of the investigated lithium DESs with respect to the choline-chloride systems, their ionic translational dynamics, quantified by the conductivity, is also significantly reduced. This again can be in principle understood when considering the strong interactions of the lithium ions. Moreover, the detected conductivity differences between these three DESs also mirror the corresponding variations of their reorientational relaxation times. Their different T_g and partly also fragility values qualitatively explain these results.

While there is a principle link of both the translational ionic and reorientational dipolar motions to the glassy dynamics, leading to similar temperature dependence, a direct

comparison of the temperature-dependent relaxation times and dc resistivities reveals some significant deviations from a perfect coupling, in particular at low temperatures. This is especially obvious for LiOTf/EG and LiOTf/Gly, in marked contrast to ethaline and glyceline²³ containing choline-chlorine instead of the lithium salts. Therefore, a revolving-door-like mechanism is not the dominant charge-transport mechanism in these materials. Just as previously reported for reline, we find a fractional DSE relation for the lithium DESs, which involves an enhancement of the ionic conductivity with decreasing temperature, finally reaching about one decade for LiOTf/EG and LiOTf/Gly. It thus seems likely that in these systems the small lithium ions find paths within the liquid structure enabling enhanced diffusion going beyond that expected for a viscous medium at low temperatures. This effect seems to be less important for LiTFSI/urea where the mentioned decoupling is less pronounced. Anyway, it should be noted that, in most of the investigated temperature ranges, the lithium DESs have conductivity values that are many decades lower than those of the corresponding choline-chloride systems with the same HBDs. As revealed by Fig. 4(a), fortunately (from an application viewpoint) these differences are strongly reduced close to room temperature which essentially can be traced back to variations in the VFT parameters describing the pronounced non-Arrhenius behavior of all these systems.

Overall, the results of the present work demonstrate the high relevance of the often-neglected glass-forming properties of DESs and of decoupling phenomena for the absolute values of their ionic dc conductivity. In addition to the present dielectric results, it certainly would be interesting to collect additional microscopic information on these materials, especially on the modification of the hydrogen-bond network by the added lithium ions and on the likely formation of ion-HBD clusters, using infrared spectroscopy and nuclear magnetic resonance measurements.

ACKNOWLEDGMENTS

This work was supported by the Deutsche Forschungsgemeinschaft (grant No. LU 656/5-1).

DATA AVAILABILITY

The data that support the findings of this study are available from the corresponding author upon reasonable request.

REFERENCES

- ¹ A. P. Abbott, G. Capper, D. L. Davies, R. K. Rasheed, and V. Tambyrajah, *Chem. Comm.* **2003**, 70.
- ² C. A. Nkuku and R. J. LeSuer, *J. Phys. Chem. B*, **111**, 13271 (2007).
- ³ Q. Zhang, K. D. O. Vigier, S. Royer, and F. Jérôme, *Chem. Soc. Rev.* **41** 7108 (2012).

- 4 Y. Dai, J. van Spronsen, G.-J. Witkamp, R. Verpoorte, and Y. H. Choi, *Anal. Chim. Acta* **766**, 61 (2013).
- 5 E. L. Smith, A. P. Abbott, and K. S. Ryder, *Chem. Rev.* **114**, 11060 (2014).
- 6 A. Paiva, R. Craveiro, I. Aroso, M. Martins, R. L. Reis, and A. R. C. Duarte, *ACS Sustainable Chem. Eng.* **2**, 1063 (2014).
- 7 M. H. Chakrabarti, F. S. Mjalli, I. M. AlNashef, M. A. Hashim, M. A. Hussain, L. Bahadori, and C. T. J. Low, *Renewable Sustainable Energy Rev.* **30**, 254 (2014).
- 8 C. J. Clarke, W. C. Tu, O. Levers, A. Bröhl, and J. P. Hallett, *Chem. Rev.* **118**, 747 (2018).
- 9 L. Millia, V. Dall'Asta, C. Ferrara, V. Berbenni, E. Quartarone, F. M. Perna, V. Capriati, and P. Mustarelli, *Solid State Ionics* **323**, 44 (2018).
- 10 A. M. Navarro-Suárez and P. Johansson, *J. Electrochem. Soc.* **167**, 070511 (2020).
- 11 B. B. Hansen, S. Spittle, B. Chen, D. Poe, Y. Zhang, J. M. Klein, A. Horton, L. Adhikari, T. Zelovich, B. W. Doherty, B. Gurkan, E. J. Maginn, A. Ragauskas, M. Dadmun, T. A. Zawodzinski, G. A. Baker, M. E. Tuckerman, R. F. Savinell, and J. R. Sangoro, *Chem. Rev.* **121**, 123 (2021).
- 12 O. E. Geiculescu, D. D. DesMarteau, S. E. Creager, O. Haik, D. Hirshberg, Y. Shilina, E. Zinigrad, M. D. Levi, D. Aurbach, and I. C. Halalay, *J. Power Sources* **307**, 519 (2016).
- 13 V. Lesch, A. Heuer, B. R. Rad, M. Winterac, and J. Smiatek, *Phys. Chem. Chem. Phys.* **18**, 28403 (2016).
- 14 H. Liang, H. Li, Z. Wang, F. Wu, L. Chen, and X. Huang, *J. Phys. Chem. B* **105**, 9966 (2001).
- 15 H. Cruz, N. Jordão, P. Amorim, M. Dionísio, and L. C. Branco, *ACS Sustainable Chem. Eng.* **6**, 2240 (2018).
- 16 H. Cruz, N. Jordao, A. L. Pinto, M. Dionisio, L. A. Neves, and L. C. Branco, *ACS Sustainable Chem. Eng.* **8**, 10653 (2020).
- 17 *Broadband Dielectric Spectroscopy*, edited by F. Kremer and A. Schönhal, (Springer, Berlin, 2002).
- 18 P. Lunkenheimer and A. Loidl, in *The Scaling of Relaxation Processes*, edited by F. Kremer and A. Loidl (Springer, Cham, 2018), p. 23.
- 19 L. Börjesson and L. M. Torell, *Phys. Rev. B* **32**, 2471 (1985).
- 20 D. R. MacFarlane and M. Forsyth, *Adv. Mater.* **13**, 957 (2001).
- 21 K. Geirhos, P. Lunkenheimer, M. Michl, D. Reuter, and A. Loidl, *J. Chem. Phys.* **143**, 081101 (2015).
- 22 P. Sippel, S. Krohns, D. Reuter, P. Lunkenheimer, and A. Loidl, *Phys. Rev. E* **98**, 052605 (2018).
- 23 D. Reuter, C. Binder, P. Lunkenheimer, and A. Loidl, *Phys. Chem. Chem. Phys.* **21**, 6801 (2019).
- 24 S. N. Tripathy, Z. Wojnarowska, J. Knapik, H. Shirota, R. Biswas, and M. Paluch, *J. Chem. Phys.* **142**, 184504 (2015).
- 25 A. Faraone, D. V. Wagle, G. A. Baker, E. Novak, M. Ohl, D. Reuter, P. Lunkenheimer, A. Loidl, and E. Mamontov, *J. Phys. Chem. B* **122**, 1261 (2018).
- 26 P. J. Griffin, T. Cosby, A. P. Holt, R. S. Benson, and J. R. Sangoro, *J. Phys. Chem. B* **118**, 9378 (2014).
- 27 K. Mukherjee, A. Das, S. Choudhury, A. Barman, and R. Biswas, *J. Phys. Chem. B* **119**, 8063 (2015).
- 28 K. Mukherjee, E. Tarif, A. Barman, and R. Biswas, *Fluid Phase Equilib.* **448**, 22 (2017).
- 29 K. Mukherjee, S. Das, E. Tarif, A. Barman, and R. Biswas, *J. Chem. Phys.* **149**, 124501 (2018).
- 30 V. Agieienko and R. Buchner, *Phys. Chem. Chem. Phys.* **22**, 20466 (2020).
- 31 R. Böhmer, M. Maglione, P. Lunkenheimer, and A. Loidl, *J. Appl. Phys.* **65**, 901 (1989).
- 32 D. Reuter, P. Münzner, C. Gainaru, P. Lunkenheimer, A. Loidl, and R. Böhmer, *J. Chem. Phys.* **154**, 154501 (2021).
- 33 P. B. Macedo, C. T. Moynihan, and R. Bose, *Phys. Chem. Glasses* **13**, 171 (1972).
- 34 S. Emmert, M. Wolf, R. Gulich, S. Krohns, P. Lunkenheimer, and A. Loidl, *Eur. Phys. J. B* **83**, 157 (2011).
- 35 In an earlier room-temperature measurement of $\sigma(\nu)$ of LiOTf/gly,¹⁵ similar behavior was found.
- 36 P. Lunkenheimer, U. Schneider, R. Brand, and A. Loidl, *Contemp. Phys.* **41**, 15 (2000).
- 37 As discussed below, upon cooling increasing deviations from the relaxation times of pure glycerol show up. Here intermolecular interactions become successively important while at elevated temperatures essentially independent single-molecule motions start to prevail.
- 38 K. Duvvuri and R. Richert, *J. Phys. Chem. B* **108**, 10451 (2004).
- 39 L.-M. Wang, Y. Tian, R. Liu, and R. Richert, *J. Phys. Chem. B* **114**, 3618 (2010).
- 40 M. Wübbenhorst and J. van Turnhout, *J. Non-Cryst. Solids* **305**, 40 (2002).
- 41 G. P. Johari and M. Goldstein, *J. Chem. Phys.* **53**, 2372 (1970).
- 42 A. Kudlik, S. Benkhof, T. Blochowicz, C. Tschirwitz, and E. A. Rössler, *J. Mol. Structure* **479**, 201 (1999).
- 43 S. Kastner, M. Köhler, Y. Goncharov, P. Lunkenheimer, and A. Loidl, *J. Non-Cryst. Solids* **357**, 510 (2011).
- 44 A. Rivera and E. A. Rössler, *Phys. Rev. B* **73**, 212201 (2006).
- 45 J. C. Dyre, *J. Appl. Phys.* **64**, 2456 (1988).
- 46 T. B. Schröder and J. C. Dyre, *Phys. Rev. Lett.* **101**, 025901 (2008).
- 47 C. Krause, J. R. Sangoro, C. Iacob, and F. Kremer, *J. Phys. Chem. B* **114**, 382 (2010).
- 48 J. R. Sangoro, C. Iacob, S. Naumov, R. Valiullin, H. Rexhausen, J. Hunger, R. Buchner, V. Strehmel, J. Kärger, and F. Kremer, *Soft Matter* **7**, 1678 (2011).
- 49 C. A. Thomann, P. Münzner, K. Moch, J. Jacquemin, P. Goodrich, A. P. Sokolov, R. Böhmer, and C. Gainaru, *J. Chem. Phys.* **153**, 194501 (2020).
- 50 For the high-frequency data of LiTFSI/urea, we found a temperature offset compared to the low-frequency measurements of order 2 K, and, consequently, these data were temperature-adjusted in order to match the low-frequency curves.
- 51 D. W. Davidson and R. H. Cole, *J. Chem. Phys.* **19**, 1484 (1951).
- 52 K. S. Cole and R. H. Cole, *J. Chem. Phys.* **9**, 341 (1941).
- 53 C. Cramer, K. Funke, M. Buscher, A. Happe, T. Saatkamp, and D. Wilmer, *Philos. Mag. B* **71**, 713 (1995).
- 54 A common definition of T_g is given by $\eta(T_g) = 10^{12}$ Pas.
- 55 C. J. Jafra, C. Bridges, L. Haupt, C. Do, P. Sippel, M. J. Cochran, S. Krohns, M. Ohl, A. Loidl, E. Mamontov, P. Lunkenheimer, S. Dai, and X.-G. Sun, *ChemSusChem* **11**, 3512 (2018).
- 56 H. Vogel, *Z. Phys.* **22**, 645 (1921).
- 57 G. S. Fulcher, *J. Am. Ceram. Soc.* **8**, 339 (1925).
- 58 G. Tammann and W. Hesse, *Z. Anorg. Allg. Chem.* **156**, 245 (1926).
- 59 C. A. Angell, in *Relaxations in Complex Systems*, edited by K. L. Ngai and G. B. Wright (NRL, Washington, DC, 1985), p. 3.
- 60 C. T. Moynihan, L. P. Boesch, and N. L. Laberge, *Phys. Chem. Glasses* **14**, 122 (1973).
- 61 M. D. Ediger, C. A. Angell, and S. R. Nagel, *J. Phys. Chem.* **100**, 13200 (1996).
- 62 J. C. Dyre, *Rev. Mod. Phys.* **78**, 953 (2006).
- 63 R. Böhmer, K. L. Ngai, C. A. Angell, and D. J. Plazek, *J. Chem. Phys.* **99**, 4201 (1993).
- 64 P. Sippel, P. Lunkenheimer, S. Krohns, E. Thoms, and A. Loidl, *Sci. Rep.* **5**, 13922 (2015).
- 65 O. S. Hammond, D. T. Bowron, and K. J. Edler, *Green Chem.* **18**, 2736 (2016).
- 66 C. A. Angell, *J. Phys. Chem. Solids* **49**, 863 (1988).
- 67 R. Böhmer and C. A. Angell, in *Disorder Effects on Relaxational Processes*, edited by R. Richert and A. Blumen (Springer, Berlin, 1994), p. 11.
- 68 This reasonably agrees with the value of $T_g = 210$ K reported for dehydrated LiOTf/Gly in Ref. 15.

- ⁶⁹ P. Lunkenheimer, S. Kastner, M. Köhler, and A. Loidl, *Phys. Rev. E* **81**, 051504 (2010).
- ⁷⁰ M. Köhler, P. Lunkenheimer and A. Loidl, *Eur. Phys. J. E* **27**, 115 (2008).
- ⁷¹ C. D'Agostino, R. C. Harris, A. P. Abbott, L. F. Gladden, and M. D. Mantle, *Phys. Chem. Chem. Phys.* **13**, 21383 (2011).
- ⁷² D. V. Wagle, G. A. Baker, and E. Mamontov, *J. Phys. Chem. Lett.* **6**, 2924 (2015).
- ⁷³ Y. Zhang, D. Poe, L. Heroux, H. Squire, B. W. Doherty, Z. Long, M. Dadmun, B. Gurkan, M. E. Tuckerman, and E. J. Maginn, *J. Phys. Chem. B* **124**, 5251 (2020).
- ⁷⁴ B. P. Jordan, R. J. Sheppardt, and S. Szwarnowski, *J. Phys. D: Appl. Phys.* **11**, 695 (1978).
- ⁷⁵ F. Kremer, A. Huwe, M. Arndt, P. Behrens, and W. Schwieger, *J. Phys. Condens. Matter* **11**, A175 (1999).
- ⁷⁶ It is more convenient to compare ρ_{dc} instead of σ_{dc} with $\langle\tau\rangle$, because both quantities have negative temperature gradient.
- ⁷⁷ E. I. Cooper and C. A. Angell, *Solid State Ionics* **18-19**, 570 (1986).
- ⁷⁸ C. M. Roland, S. H. Bielowka, M. Paluch, and R. Casalini, *Rep. Prog. Phys.* **68**, 1405 (2005).
- ⁷⁹ G. P. Johari and O. Andersson, *J. Chem. Phys.* **125**, 124501 (2006).
- ⁸⁰ S. H. Bielowka, T. Psurek, J. Ziolo, and M. Paluch, *Phys. Rev. E* **63**, 062301 (2001).
- ⁸¹ As pointed out in Ref. 78, unfortunately, in literature there is no consistent use of the term "Debye-Stokes-Einstein relation" and it is also often applied to an equation implying the proportionality $D_r \propto T/\eta$, where D_r is the rotational diffusion coefficient and η the viscosity.